Occurrence of the Gomphotherium angustidens *group in China, based on a revision of* Gomphotherium connexum *(Hopwood, 1935) and* Gomphotherium shensiensis *Chang and Zhai, 1978: continental correlation of* Gomphotherium *species across the Palearctic*

Shi-Qi Wang, Jaroon Duangkrayom & Xiang-Wen Yang

Paläontologische Zeitschrift
Scientific Contributions to Palaeontology

ISSN 0031-0220

Paläontol Z
DOI 10.1007/s12542-015-0270-8

Springer

Paläontol Z
DOI 10.1007/s12542-015-0270-8

RESEARCH PAPER

Occurrence of the *Gomphotherium angustidens* group in China, based on a revision of *Gomphotherium connexum* (Hopwood, 1935) and *Gomphotherium shensiensis* Chang and Zhai, 1978: continental correlation of *Gomphotherium* species across the Palearctic

Shi-Qi Wang[1,2,3] · **Jaroon Duangkrayom**[1,4,5] · **Xiang-Wen Yang**[1,4]

Received: 6 June 2014 / Accepted: 22 May 2015

Abstract In this paper, we restudy previously reported material of *Gomphotherium connexum* and *G. shensiensis* from China. *G. connexum* is characterized by the strong posterior pretrite central conules of the upper molars, which are larger than the corresponding anterior ones (at least in the second loph), the narrow interloph(id)s, the high central conules, and the narrow contour of m3. *Gomphotherium* cf. *shensiensis* (here is attributed to *G. connexum*) from the Junggar Basin is more derived than the type material of *G. connexum* in larger size and heavier cementum. *G. connexum* is very similar to *G. angustidens*, which was widely distributed in the Middle Miocene (MN6–8) of Europe. *Gomphotherium shensiensis* (here is attributed to *G.* cf. *subtapiroideum*) shows crest-like elements in the teeth crowns. The posttrite lophs are subdivided and anteroposteriorly compressed, and the interlophs are relatively anteroposteriorly wide. These features are similar to *G. subtapiroideum*, which occurred in the later Early Miocene to the earlier Late Miocene (MN5–9) of Europe. This revision of Chinese *Gomphotherium* demonstrates strong similarities in *Gomphotherium* species between eastern and western Eurasia, representing a continental diffusion of *Gomphotherium* species across the Palearctic region.

Keywords *Gomphotherium angustidens* · *Gomphotherium subtapiroideum* · Systematics · Proboscidean · Miocene

Kurzfassung In dieser Studie re-evaluieren wir bereits früher beschriebenes Material von *Gomphotherium connexum* und *G.* „*shensiensis*“ aus China. *Gomphotherium connexum* ist durch stark ausgeprägte, posteriore prätrite Zentral-Conuli der oberen Molaren, die (zumindest am zweiten Joch) größer sind als die entsprechenden anterioren Gegenstücke, durch anteroposterior komprimierte Täler, hohe zentrale Conuli sowie durch das schmale Profil des m3 gekennzeichnet. *Gomphotherium* cf. „*shensiensis*“ (wird hier *G. connexum* zugeschrieben) aus dem Junggar Basin ist im Vergleich zu *G. connexum* stärker abgeleitet, was sich in einer Zunahme der allgemeinen Körpergröße und in stärker ausgeprägtem Zahnzement im Vergleich zum Typus-Material äußert. *Gomphotherium connexum* ähnelt *G. angustidens*, einem im mittleren Miozän (MN6–8) in Europa weit verbreiteten Taxon, stark. *Gomphotherium* „*shensiensis*“ (wird hier *G.* cf. *subtapiroideum* zugeschrieben) zeigt eher kammartige Elemente in seinen Zahnkronen. Die postriten Zahnjoche sind unterteilt und

✉ Shi-Qi Wang
wangshiqi@ivpp.ac.cn

Jaroon Duangkrayom
jduangkrayom@gmail.com

Xiang-Wen Yang
344490433@qq.com

[1] Key Laboratory of Vertebrate Evolution and Human Origins of Chinese Academy of Sciences, Institute of Vertebrate Paleontology and Paleoanthropology, Chinese Academy of Sciences, Beijing 100044, China

[2] CAS Center for Excellence in Tibetan Plateau Earth Sciences, Beijing 100101, China

[3] Key Laboratory of Economic Stratigraphy and Palaeogeography, Chinese Academy of Sciences (Nanjing Institute of Geology and Palaeontology), Nanjing 210008, China

[4] University of the Chinese Academy of Sciences, Beijing 100049, China

[5] Northeastern Research Institute of Petrified Wood and Mineral Resources, Nakhon Ratchasima Rajabhat University, Nakhon Ratchasima 30000, Thailand

Published online: 11 June 2015

anteroposterior komprimiert, während die Täler anteroposterior relativ breit sind. Diese Eigenschaften sind ähnlich wie *G. subtapiroideum*, das ebenfalls im späteren frühen Miozän bis früheren späten Miozän (MN5–9) Europas vorkommt. Die Revision von *Gomphotherium* aus China lässt starke Ähnlichkeiten bei *Gomphotherien*-Arten zwischen dem östlichen und westlichen Eurasien erkennen, was eine kontinentale Verbreitung von *Gomphotherium*-Spezies quer durch die paläarktische Region zeigt.

Schlüsselwörter *Gomphotherium angustidens* · *Gomphotherium subtapiroideum* · Systematik · Proboscidea · Miozän

Abbreviations

IVPP	Institute of Vertebrate Paleontology and Paleoanthropology, Beijing, China
MNHN	Muséum national d'Histoire naturelle, Paris, France
NHMW	Naturhistorisches Museum Wien, Vienna, Austria
PMU	Palaeontological Museum, Uppsala, Sweden

Introduction

The genus *Gomphotherium* is an important taxon of Elephantoidea Gray, 1821 (Tobien 1972, 1973; Tassy 1985, Shoshani and Tassy 2005). *Gomphotherium connexum* and *G. shensiensis* are two members of the genus known only from China. The type material of *G. connexum* was published by Hopwood (1935), and it was the first gomphotheriid species named in China. The type locality is Diaogou [=Tiao Kou (Hopwood 1935)], Huangzhong County, Qinhai Province, in the Xianshuihe [=Hsienshuiho (Young and Bian 1937)] Formation. However, this species appears to be rather isolated. Besides a small amount of additional material from the type locality (Qiu et al. 1981), *Gomphotherium* cf. *connexus* has only been reported from Qinan, Gansu Province (Zhai 1961). However, the material, a left m2, is in fact not a *Gomphotherium,* but a *Choerolophodon* (Tobien et al. 1986). The type material of *G. shensiensis* was described by Chang and Zhai (1978), represented by a relatively complete cranium. The type locality is Lengshuigou, Lintong County, Shaanxi (=Shensi) Province, in the Lengshuigou Formation (Chang and Zhai 1978). The age is MN6 (Qiu and Qiu 1995). Similarly, this is also an isolated species: *Gomphotherium* cf. *shensiensis* has only been reported from the Halamagai Formation of the Junggar Basin, Xinjiang Province (Chen 1988). The age is also MN6 (Ye et al. 2012).

For a long time, *Gomphotherium* Burmeister, 1837 was not a well-defined taxon. It was regarded as the senior synonym of *Trilophodon* Falconer, 1857, *Bunolophodon* Vacek, 1877, *Tetrabelodon* Cope, 1884, *Serridentinus* Osborn, 1923, *Tatabelodon* Frick, 1933, *Ocalientinus* Frick, 1933, and *Trobelodon* Frick, 1933 (Tobien 1972), and many taxa were established under these junior synonyms (Tobien 1972). For example, Osborn (1936) listed 60 species in these genera. In China, Hopwood (1935) listed six species of *Trilophodon* and *Serridentinus* (including species from Mongolia). Chow and Zhang (1974) listed 16 species of *Gomphotherium* and *Serridentinus*.

Tobien (1973) revised the genus *Gomphotherium*. He included all the Eurasian and African species of *Gomphotherium* in the *G. angustidens* group and included all the American species in *G. productum*. Tobien et al. (1986) also revised the Chinese *Gomphotherium*. Only three species of *Gomphotherium* (*G. connexum*, *G. wimani*, and *G. shensiensis*) were retained. Tobien's *G. angustidens* group is a *Formenkreis* containing many morphological types. It is necessary to subdivide this group further and to discuss the relationships between different types within the group. Tassy (1985) divided *Gomphotherium* into the *G. annectens* group and the *G. angustidens* group. The former (including *G. annectens*, *G. sylvaticum*, and *G. cooperi*) exhibits more plesiomorphies than other species of *Gomphotherium*, such as small central conules, incomplete fourth loph(id)s in M3 or m3, and relatively wide interloph(id)s (Tassy 1985). The latter [including *G. angustidens*, *G. inopinatum*, and *G. angustidens* of subtapiroid form (=*G. subtapiroideum*)] is not equal to the *G. angustidens* group defined by Tobien (1973), and is derived from the *G. annectens* group (Tassy 1985, 2014). Tassy's framework has been used in subsequent studies. On the basis of this framework, new species have been established (e.g. *G. sylvaticum* Tassy, 1985 and *G. hannibali* Welcomme, 1994), and some old names have been revived, such as *G. subtapiroideum* (Schlesinger, 1917), *G. mongoliense* (Osborn, 1924), and *G. praetypicum* (Tasnádi Kubacska, 1939); however, *G. pygmaeum* (Depéret, 1897) remains controversial (Welcomme 1994; Göhlich 1998, 2007, 2010; Gasparik and Markov 2009; Sanders et al. 2010; Tassy et al. 2013).

After Tobien et al. (1986) revised the genus *Gomphotherium* in China, there were few studies on Chinese *Gomphotherium*. Subsequently, no other species of *Gomphotherium* were introduced until one of the authors (S-QW) recently studied *G. inopinatum* from the Lower Miocene of the Linxia Basin, which is the most primitive species so far known in China (Wang 2014). In the same paper, the author considered that *G. connexum* is closely related to the European *G. angustidens*, while *G. shensiensis* is possibly synonymized with *G. subtapiroideum*. As space was limited, the discussion in that paper was very brief. Herein, we will

further discuss the material relevant to *G. connexum* and *G. shensiensis*. This is also an intensive study of Chinese *Gomphotherium*. We hope that this work will improve our understanding of the phylogeny and global distribution of *Gomphotherium* in the eastern part of the Palearctic region.

Materials and methods

All the material presented herein is housed in the IVPP. The odontological and osteological terminology and the measurements used follow Tassy (2013, 2014) (Fig. 1).

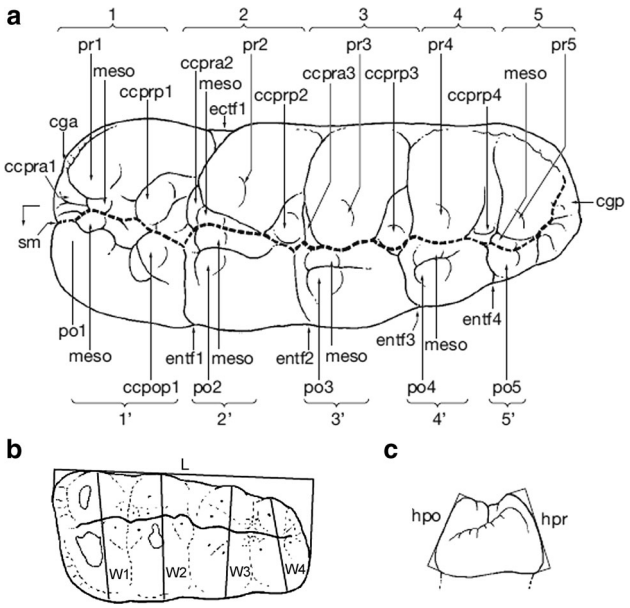

Fig. 1 Tooth nomenclature and measurements (after Tassy 2014, Figs. 2B, 3F, K). **a** Tooth nomenclature illustrated on a right m3, occlusal view; **b** length and width measurements illustrated on a left M3, occlusal view; **c** height measurements on a molar, anterior view. *1*, *2*, *3*, *4*, and *5* first, second, third, fourth, and fifth pretrite half lophids; *1′*, *2′*, *3′*, *4′*, and *5′* first, second, third, fourth, and fifth posttrite half lophids; *ccpop1* first posterior posttrite central conule; *ccpra1* first anterior pretrite central conule (paraconid or paracristid); *ccpra2* second anterior pretrite central conule (mesoconid); *ccpra3* third anterior pretrite central conule; *ccprp1* first posterior pretrite central conule (protoconulid); *ccprp2*, *3*, and *4* second, third, and fourth posterior pretrite central conules; *cga* anterior cingulid; *cgp* posterior cingulid; *ectf1* ectoflexid of the first interlophid; *entf1*, *2*, *3*, and *4* entoflexids of first, second, third, and fourth interlophids; *meso* mesoconelet of each half lophid; *po1* main cuspid of the first posttrite half lophid (metaconid); *po2* main cuspid of the second posttrite half lophid (entoconid); *po3* main cuspid of the third posttrite half lophid (hypoconulid); *po4* and *5* main cuspids of the fourth and fifth posttrite half lophids; *pr1* main cuspid of the first pretrite half lophid (protoconid); *pr2* main cuspid of the second pretrite half lophid (hypoconid); *pr3* main cuspid of the third pretrite half lophid (postentoconulid); *pr4* and *5* main cuspids of the fourth and fifth pretrite half lophids; *sm* median sulcus; *L* length; *W* maximal width; *W1*, *2*, *3*, and *4* width at the first, second, third, and fourth lophs; *hpr* height of the pretrite side; *hpo* height of the posttrite side

Measurements were obtained using calipers, and measured in mm.

Systematic paleontology

Order Proboscidea Illiger, 1811
Family Gomphotheriidae Hay, 1922
Genus *Gomphotherium* Burmeister, 1837
Gomphotherium connexum (Hopwood, 1935)
Figures 2 and 3; Table 1

Trilophodon connexus Hopwood, 1935: pl. V, Figs. 1, 2
non *Gomphotherium* cf. *connexus* (Hopwood, 1935): Zhai 1961, pl. I, Fig. 2

Gomphotherium connexus (Hopwood, 1935): Chow and Zhang 1974, Fig. 19; pl. I, Figs. 1, 2

Gomphotherium connexus (Hopwood, 1935): Qiu et al. 1981, pl. I, Fig. 9

Gomphotherium connexum (Hopwood, 1935): Tobien et al. 1986, Figs. 2–6

Gomphotherium cf. *shensiensis* Chang and Zhai, 1978: Chen 1988, pl. I, Figs. 1–3; pl. II, Figs. 1–3

Gomphotherium sp.: Chen 1988, pl. I, Figs. 1, 2

Holotype PMU-M 3469, a left hemimandible carrying a moderately worn m2 and a slightly worn, erupting m3. The alveolus of m1 has not been entirely absorbed. The description and photograph herein are based on a cast in IVPP (IVPP RV35015), figured by Hopwood (1935, pl. V, Fig. 1).

Paratypes PMU-M 3047, a left P4; PMU-M 3045 [a cast (IVPP RV35D49) is in the IVPP, on which the description is based], a left M3; PMU-M 3049, a left hemimandible carrying p3, dp4, and m1; PMU-M 3046, a right p4; PMU-M 3048, a left m2.

Type locality and horizon Diaogou, Huangzhong County, Qinhai Province, Xianshuihe Formation, late Early Miocene (there is no precise dating on the Diaogou locality, and here we estimate the age to be the late Early Miocene because the type material is slightly more primitive than *G. connexum* from Halamagai Formation, MN6, see below) (Hopwood 1935; Qiu et al. 1981; Tobien et al. 1986).

Stratigraphic and geographic distribution Eastern Asia, later Early Miocene (type locality) to Middle Miocene (Halamagai Formation, MN6, Ye et al. 2012).

Referred material IVPP V8568, a fragmented left mandibular tusk; V8573, V8574, and V8576, three left M3; V8572, a right M3; V8569, a left dp4; V8575, and V18701, two left m3; V8571, a right m3; all from the Junggar Basin,

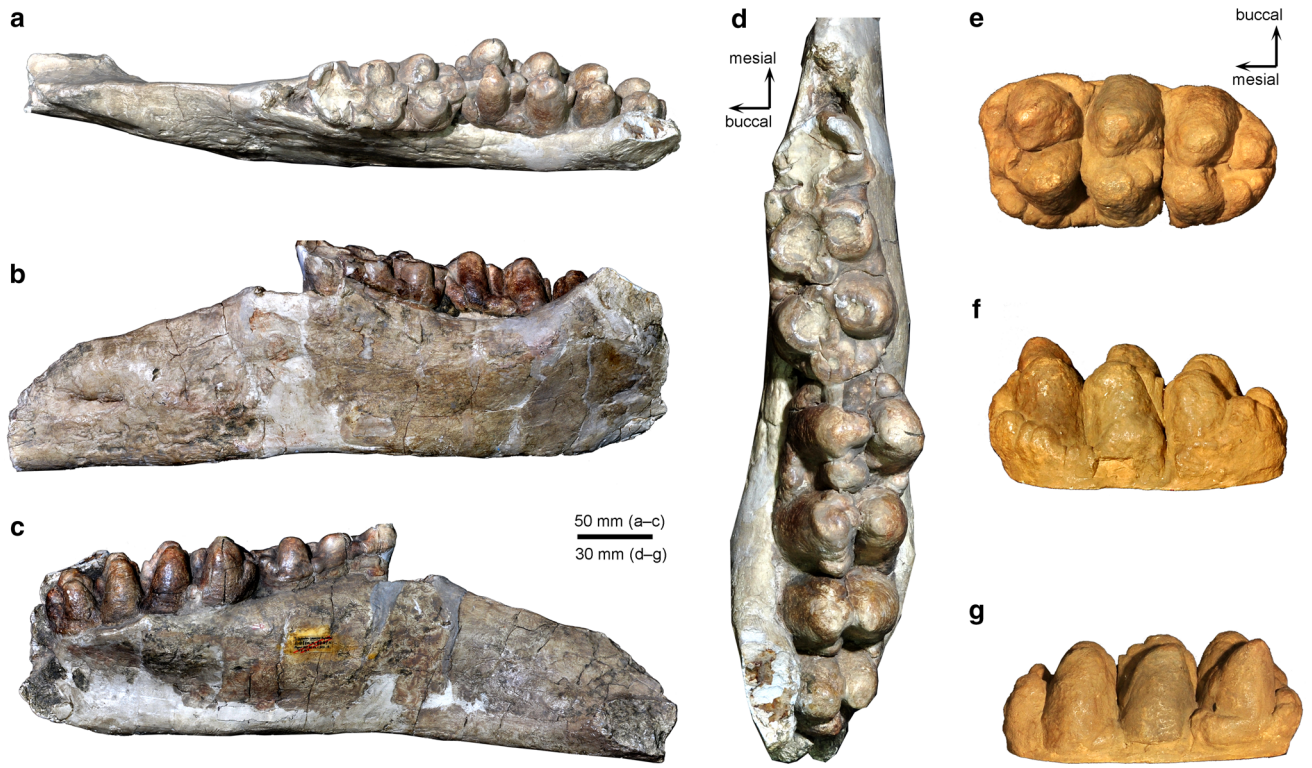

Fig. 2 Type material of *Gomphotherium connexum* from Diaogou. **a–c** Dorsal, lateral, and medial views of the mandible IVPP RV35015, a cast of the holotype PMU-M 3469; **d** occlusal view of m2–m3 teeth row of the holotype IVPP RV35015; **e–g** occlusal, lingual, and buccal views of the left M3 (IVPP RV35D49), the cast of PMU-M 3045, the paratype from Diaogou

Halamagai Formation, Middle Miocene, MN6 (Chen 1988; Ye et al. 2012).

Description of the selected specimen of the type material the holotype (Fig. 2a–d), PMU-M 3469, is the mandibular corpus and the posterior part of the mandibular symphysis. The mandibular corpus is narrow and high, and the greatest height of the corpus is at the level of the anterior end of the alveolus of the missing m1. The midline of the mandibular symphysis is downwardly deflected from the corpus at an angle of about 24° (this measurement see Göhlich 1998, Fig. 66). The posterior border of the symphysis is distant from the anterior end of the m1 alveolus at a distance of 116 mm. The rounded posterior mental foramen is at the level of the m1 alveolus and the anteroposteriorly elongated anterior mental foramen is at the level of the posterior border of the symphysis. The remaining alveolus of the mandibular tusk at the anterior cross-section is small and oval. The long axis of the incisive alveolus has a dorsolateral–ventromedial orientation.

The m2 (Fig. 2d) is trilophodont with a strong posterior cingulid. The first and second posterior pretrite central conules are high (in buccal view), larger than the corresponding anterior central conules, and tend to invade into the corresponding posttrite half interlophids. In some cases, the posterior pretrite central conules are subdivided (e.g. PMU-M 3048, Tobien et al. 1986, Fig. 6). The third posterior pretrite central conule is weak or absent. Both pretrite and posttrite mesoconelets are small and bud-like.

The m3 (Fig. 2d), PMU-M 3469, possesses four lophids and a posterior cingulid. It is very slender and the widest part of the tooth is at the second lophid. The first pretrite trefoil is symmetrical with large and subdivided anterior and posterior central conules and a small mesoconelet. The second and third posterior pretrite central conules are high (in buccal view), larger than the corresponding anterior central conules, and tend to invade into the corresponding posttrite half interlophids. The fourth posterior pretrite central conule is missing. The pretrite mesoconelets of the second, third, and fourth lophid are small and anteriorly positioned. The posttrite half lophids are simple. Posttrite central conules are missing, and posttrite mesoconelets are absent. There is a single central conelet forming a "talonid" at the posterior end of the tooth. Cingulids are developed on the anterior and posterior ends, the ecto- and entoflexids of the first interlophid of the tooth. Several small conules are developed on the ecto- and entoflexids of the first interlophid.

The M3 (Fig. 2e–g), PMU-M 3045, is fairly small with three complete lophs and an incipient fourth loph. The

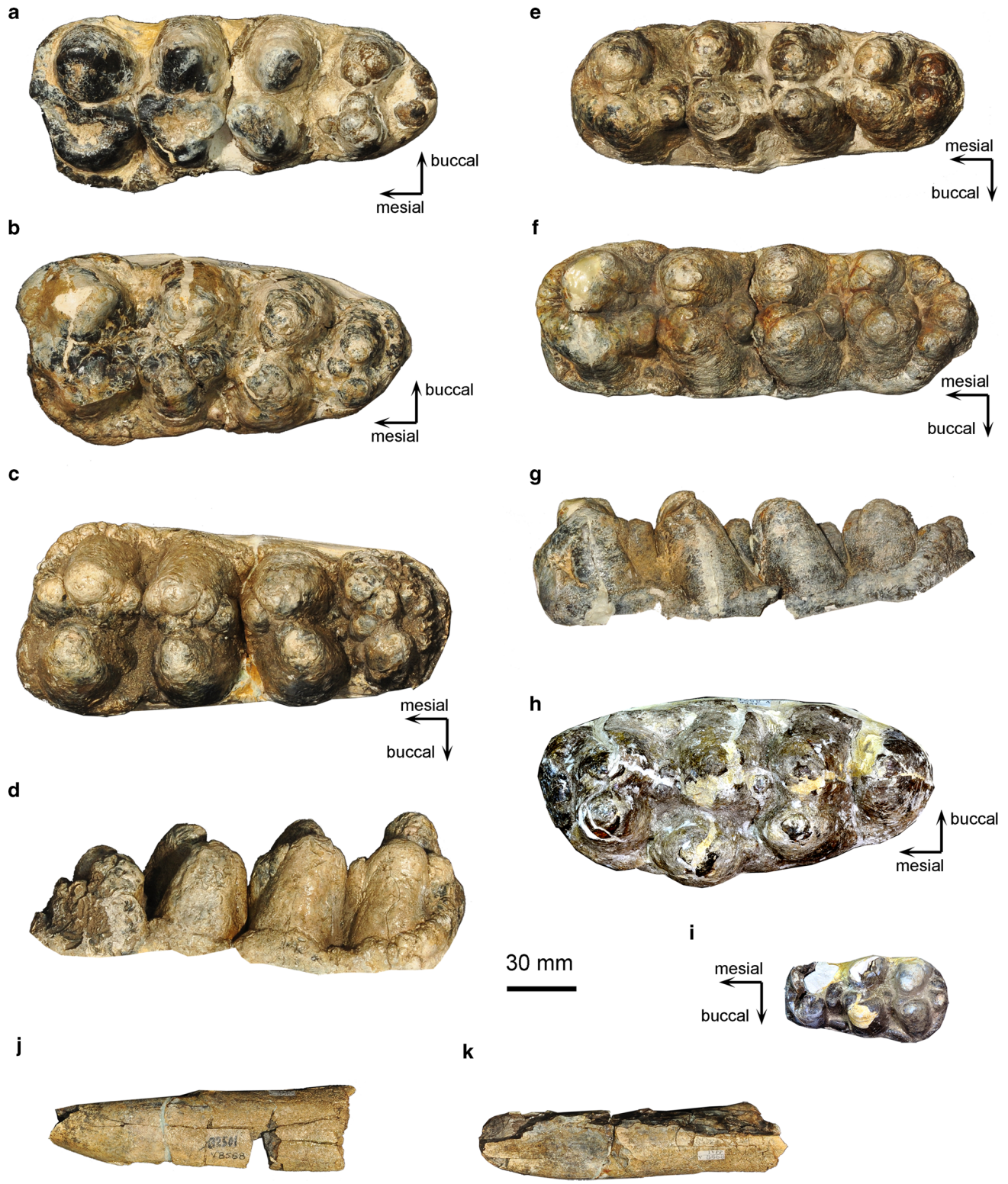

Fig. 3 *Gomphotherium connexum* from the Junggar Basin, Halamagai Formation. **a** IVPP V8576, left M3, in occlusal view; **b** IVPP V8573, left M3, in occlusal view; **c** IVPP V8572, right M3, in occlusal view; **d** IVPP V8572, in lingual view; **e** IVPP V8575, left m3, in occlusal view; **f** IVPP V18701, left m3, in occlusal view; **g** IVPP V18701, in lingual view; **h** IVPP V8571, right m3, in occlusal view; **i** IVPP V8509, left dp4, in occlusal view; **j** IVPP V8568, fragments of a left mandibular tusk, in lateral view; **k** IVPP V8568, in dorsal view

Table 1 Cheek teeth measurements (in mm, after Tassy 2014) of *Gomphotherium connexum* and *G.* cf. *subtapiroideum*

No.	Species	Locality	Locus	*L*	*W*	*W1*	*W2*	*W3*	*W4*	*hpo*	*I* = *W*/*L*
V5576	*G.* cf. *subtapiroideum*	Heijiagou	r. M1	94.74	54.95	50.7	54.34	54.95		43.33$^{(3)}$	0.58
V3084	*G.* cf. *subtapiroideum*	Lengshuigou	l. M2	121+	74.5+	–	–	–		–	–
V3084	*G.* cf. *subtapiroideum*	Lengshuigou	r. M2	130.5	79	75.5	–	70.5		–	0.61
RV35049	*G. connexum*	Diaogou	r. M3	120.01	62.08	62.08	60.00	57.11		41.26$^{(2)}$	0.52
V8572	*G. connexum*	Junggar	r. M3	186.93	83.78	83.78	76.75	72.1	63.36	51.28$^{(2)}$	0.45
V8573	*G. connexum*	Junggar	l. M3	170.72	82.74	82.74	77.1	72.31	50.86	50.41$^{(3)}$	0.48
V8576	*G. connexum*	Junggar	l. M3	176.15	74.93	74.93	71.58	67.61	57.56	50.70$^{(3)}$	0.43
V8574	*G. connexum*	Junggar	l. M3	–	–	–	–	67.24	59.95	57.15$^{(3)}$	–
V3084	*G.* cf. *subtapiroideum*	Lengshuigou	l. M3	169	85	85	83.5	68.5	55.5	–	0.50
V3084	*G.* cf. *subtapiroideum*	Lengshuigou	r. M3	175	78.5	78.5	77	73.5	62	–	0.45
V8569	*G. connexum*	Junggar	l. dp4	71.83	37.82	–	–	37.82		33.12$^{(2)}$	0.53
RV35015	*G. connexum*	Diaogou	l. m2	103.49	45.13	38.97	45.13	50.23			0.44
RV35015	*G. connexum*	Diaogou	l. m3	148.52	51.45	50.68	51.45	–	–	46.72+$^{(2)}$	0.35
V18701	*G. connexum*	Junggar	l. m3	191.09	68.1	68.1	65.22	67.31	65.05	54.14$^{(2)}$	0.36
V8571	*G. connexum*	Junggar	r. m3	172.02	76.04	68.37	76.04	67.32	52.38	58.51$^{(2)}$	0.44
V8575	*G. connexum*	Junggar	l. m3	169.99	64.27	57.31	64.27	58.47	51.31	58.03$^{(1)}$	0.38

L length, *W* maximal width, *W1*, *2*, *3*, and *4* width at the first, second, third, and fourth loph(id), *I* index, *hpo* height of the posttrite side [numbers in brackets indicate the loph(id) from which the measurement was taken]

cusps are bulky and the interlophs are narrow. The first anterior and posterior pretrite central conules are of equal dimensions, but the first pretrite mesoconelet is very small or absent. The second pretrite trefoil is asymmetrical with a larger, bisubdivided posterior central conule. The second pretrite mesoconelet is very small, anteriorly positioned, and close to the second anterior pretrite central conule. The third pretrite trefoil is incomplete. The third posterior pretrite central conule and the third pretrite mesoconelet are absent. The third anterior pretrite central conule is present. Posttrite mesoconelets are rather small and bud-like. Posttrite central conules are missing except for a small second posterior posttrite central conule is present. A strong anterior cingulum is developed and extends to the lingual and buccal sides of the first pretrite half loph.

Description of referred material from the Halamagai Formation the anterior segment of the lower permanent tusk (V8568, Fig. 3j, k) is relatively slender. It is so fragmentary that the shape of the cross-section and the presence of longitudinal furrows are unknown (the medial side of the tooth is severely damaged and the cross-section is incomplete). It is slightly tapered and rounded apically. The remaining length is 173.5 mm and the remaining height is 50 mm. The dorsal wear facet is oval. At the tip of the wear facet, it seems to be slightly concave (although largely damaged). The length of the wear surface is 79 mm.

All of the four M3 (Fig. 3a–d) have three complete lophs and a more or less developed fourth loph and a posterior cingulum, with the first loph being wider than the others (not known in the severely damaged V8574). In all specimens, the main cusps of the pretrite and posttrite half lophs are bulky and interlophs are anteroposteriorly narrow. The pretrite trefoils are complete on the first two lophs. The first anterior pretrite central conules are always large. In the first loph the anterior pretrite conules are slightly larger than or of equal size to the corresponding posterior ones. In all specimens, the second pretrite trefoils are asymmetrical and the posterior central conules are always larger than the corresponding anterior ones. In V8572 (Fig. 3c) and V8573 (Fig. 3b), the second posterior pretrite central conules are subdivided into two cusps. In all specimens, the third posterior pretrite central conules are missing. In all specimens, each pretrite or posttrite half loph has a single pretrite or posttrite mesoconelet (at least in the anterior three lophs). The first pretrite mesoconelets are small, and those of the second and third lophs are anteriorly positioned, close to the corresponding anterior pretrite central conules. In V8572 (Fig. 3c) and V8573 (Fig. 3b), the third pretrite mesoconelet is fused to the corresponding anterior pretrite central conule. In all specimens, the posttrite mesoconelets are small and bud-like, and posttrite central conules are almost missing, except that a weak second posterior posttrite central conule is observed in V8576 (Fig. 3a). The development of the fourth loph is variable, and the conelets of the fourth loph are irregularly arranged. A strong anterior cingulum is developed and extends to the lingual and buccal sides of the first pretrite half loph. Relatively strong cementum is in all valleys (especially in the posterior valleys) of V8573 (Fig. 3b) and V8576 (Fig. 3a).

A left dp4 (V8569, Fig. 3i) is composed of three lophids that increase in width from anterior to posterior. The first posttrite half lophid and the second posttrite main cuspid are broken. The first interlophid is anteroposteriorly wider than the second one. The first pretrite mesoconelet and the main cuspid are equal in size. Although the first anterior pretrite central conule is large, the corresponding posterior one is even larger. The second pretrite mesoconelet is large and anteriorly positioned. Both the second anterior and the posterior pretrite central conules are small. The second posttrite mesoconelet is smaller than the corresponding main cuspid and no accessory central conules are visible. The third lophid is strongly chevron-shaped. No accessory central conules are visible on both the third pretrite and the third posttrite half lophids. The third posttrite mesoconelet is small and bud-like. Cingulids are present on the anterior and posterior ends and the buccal margin. Cementum is weak.

Three m3 were available for study. V8575 and V18701 (Fig. 3e–g) are narrow, long with four lophids plus a strong posterior cingulid. The widths of the first and second lophids are almost equal. All the cuspids are bulky. In the first three lophids, the posterior pretrite central conules are far larger than the corresponding anterior ones. In V8575 (Fig. 3e), the first and second posterior pretrite central conules are subdivided into a small anterior conule and a large posterior one. In V18701 (Fig. 3f), the first posterior pretrite central conule is subdivided into three conules, but the second posterior pretrite central conule is not subdivided. In V8575 (Fig. 3e), the second and third anterior pretrite central conules are almost absent. In the first three lophids, each pretrite or posttrite half lophid has a single pretrite or posttrite mesoconelet. The first pretrite mesoconelet is small, and the second and third pretrite mesoconelets are anteriorly positioned. The first three posttrite half lophids lack central conules and the posttrite mesoconelets are smaller than the corresponding main cuspids. In V8575 (Fig. 3e), both the pretrite and the posttrite mesoconelets are not clearly separated from the main cuspids, but they are clearly separated in V18701 (Fig. 3f). The fourth lophid is strongly chevron-shaped. The posterior cingulid is composed of a few (in V8575, Fig. 3e) or more (in V18701, Fig. 3f) conelets and it is missing from either the buccal or lingual margin of the tooth. Cementum is strongly developed. V8571 (Fig. 3h) is a right m3 that is possibly somewhat abnormal. It is composed of four lophids. The second lophid is much wider than the others, from which we determine it to be a lower rather than an upper third molar. The fourth lophid is only composed of a large single conelet. Most of the secondary structures are not clear as a result of both abnormality and damage. However, the first and second posterior pretrite central conules are larger than the corresponding anterior ones.

Discussion the type material of *G. connexum* is rather small-sized. The dimensions of M3 (paratype) reach the lower boundary of *G. angustidens* from En Péjouan, France, and *G. subtapiroideum* from Sandelzhausen, Germany (Fig. 4). However, m3 and M3 are longer (not wider) than *G. annectens* from Banjôbora, Japan (Fig. 4). As Tassy et al. (2013) pointed out, size alone is not a sufficient taxonomic criterion. The M3 of female *G. angustidens* from En Péjouan has a length only 70 % of that of males (Tassy 2014). The minimum M3 length of *Platybelodon grangeri* from Linxia is only 72 % of the maximal M3 length (Wang et al. 2013). Therefore, the small dimensions also cannot be regarded as a diagnostic character of *G. connexum*.

Hopwood (1935) created the specific name *Trilophodon connexus* because subdivision of pretrite central conules is present on the upper molar, but not on the lower molar, representing, in his view, an intermediate form between *Trilophodon* and *Serridentinus*. Currently, subdivision of the pretrite central conules is not regarded as a stable feature for diagnosis of gomphotheriid taxa. Subdivision of pretrite central conules is possibly present on a left tooth, but absent on the corresponding right one (Tassy 2014).

Hopwood (1935) also considered the teeth of *G. connexum* and *G. cooperi* from Bugti to be highly similar. However, in the lower molars of *G. cooperi*, the second anterior pretrite central conule is absent (Osborn 1932) (the first anterior pretrite central conule of lower molars is always present in any gomphotheriid taxon), whereas in the type specimens of *G. connexum*, although small, this conule is present on the second lophid of the m3. More importantly, the second posterior pretrite central conule of the upper molars is very small or absent in *G. cooperi* (Osborn 1932), but is large (and subdivided) in the M3 of *G. connexum*. The interloph(id)s of *G. cooperi* are anteroposteriorly wider than those of *G. connexum* (Osborn 1932). More broadly, relatively small anterior pretrite central conules of the lower molars and relatively small posterior pretrite central conules of the upper molars, and relatively anteroposteriorly wide interloph(id)s are common features of members of the *G. annectens* group (Tassy 1985). The type material of m3 of *G. connexum* has a complete fourth lophid rather than an incomplete fourth lophid in the members of the *G. annectens* group. Thus, despite the small dimensions, *G. connexum* cannot be placed in the *G. annectens* group that includes *G. cooperi*.

Hopwood (1935) did not compare *G. connexum* with *G. angustidens*, which is very similar to *G. connexum*. Tobien et al. (1986) considered *G. connexum* to be one of the *angustidens* population or *angustidens Formenkreis*. This is true, and here we should point out that, even compared with *G. angustidens* s. s. from Simorre and En Péjouan, the similarity is still high, especially in the strong posterior

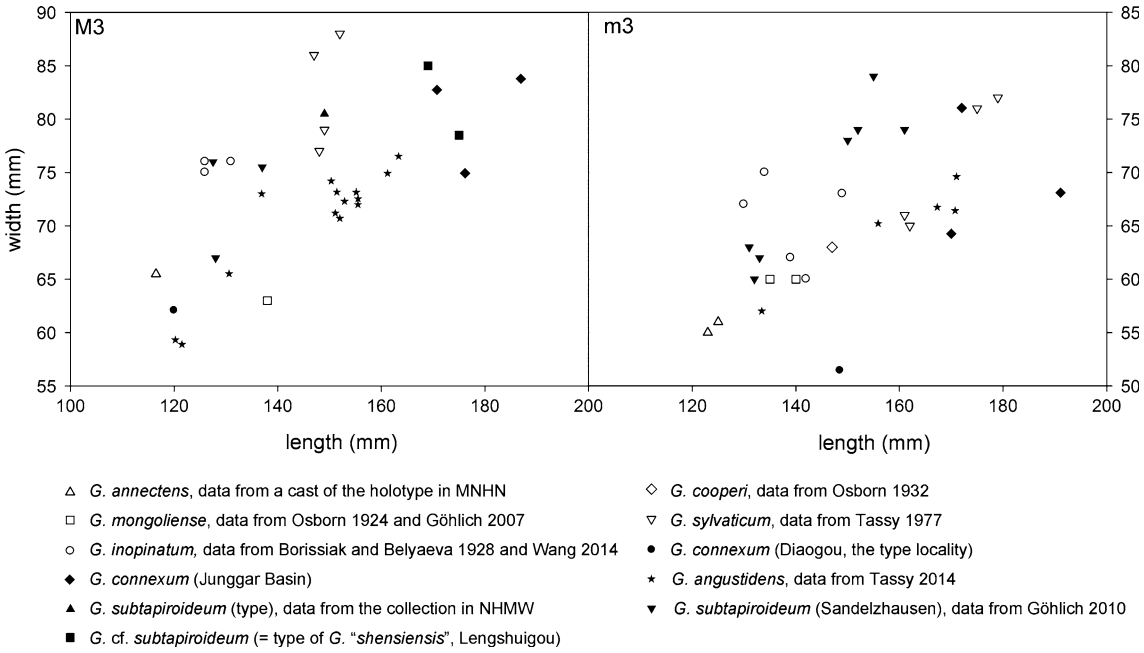

Fig. 4 Bivariate plots of M3 and m3 measurements of the *Gomphotherium annectens* group and the *Gomphotherium angustidens* group

pretrite central conules of the upper molar that are larger than the corresponding anterior ones (at least in the second loph). Other similarities are the anteroposteriorly compressed interloph(id)s, high central conules, narrow contour of m3, and potentially a concave wear facet on the tip of the dorsal facet of the lower tusks. The differences between the two are the narrower m3 (except for the potentially abnormal V8571, see Fig. 4) and smaller, lower posttrite mesoconelets in *G. connexum*, thus herein we regard *G. connexum* as a valid species. The high similarity indicates that *G. connexum* is possibly a close relative of *G. angustidens*, thus should also be a member of *G. angustidens* group. *Gomphotherium angustidens* was widely distributed in the Middle Miocene of Europe (MN 6–8, Tassy 2014). Perhaps *G. connexum* represents a phylogenetically related species of *G. angustidens* that penetrated into the eastern part of the Palearctic.

Chen (1988) described *Gomphotherium* cf. *shensiensis* and *Gomphotherium* sp. from the Middle Miocene Halamagai Formation of the Junggar Basin which we identify here as *G. connexum*. The specimens of M3 of the Junggar material vary in dimensions (Fig. 4), in shape, and in the development of cementum (Fig. 3a–d). However, the basic morphology of these M3 from the Junggar Basin is consistent. In the second loph, the posterior pretrite central conule is larger than the corresponding anterior ones [this feature is clearer in IVPP V8572 (Fig. 3c) than that in IVPP V8576 and 8573 (Fig. 3a, b)]. The interlophs are anteroposteriorly narrow. The posttrite mesoconelets are low and small. These features are identical to the type material of *G. connexum*. The specimens of m3 of the Junggar material are also similar to the type specimen in that it has strong and high posterior pretrite central conules, small posttrite mesoconelets, and a narrow contour (Fig. 3e–g). Chen (1988) also considered that these specimens show similarities to *G. connexum*. However, she did not attribute them to *G. connexum* because of their large size and small width to length ratio (Fig. 4). As has been discussed, size alone is not sufficient for taxonomic diagnosis, and shape can also be highly variable within a species. The only known M3 of the type material is actually very small, and may be an extreme case. The type m3 is not much smaller than the m3 in the Junggar material. The range of variation of the M3 of *G. connexum* is similar to that of *G. angustidens* from En Péjouan (Fig. 4). The Junggar material shows some more derived features than the type material, such as the larger size and heavier cementum, possibly because the Junggar material is geologically younger. Conversely, in the type specimen of *Gomphotherium shensiensis* (Chang and Zhai, 1978), although the dimensions of its M3 fall into the range of the Junggar material (Fig. 4), the posttrite half lophs are anteroposteriorly compressed, leaving anteroposteriorly wider interlophs, and the posterior pretrite central conules are much smaller than the corresponding anterior ones (see below), very different from the Junggar material. Therefore, we attribute these Junggar specimens to *G. connexum* rather than to *G.* cf. *shensiensis*.

Gomphotherium cf. *subtapiroideum* (Schlesinger, 1917)
Figures 5 and 6; Tables 1 and 2

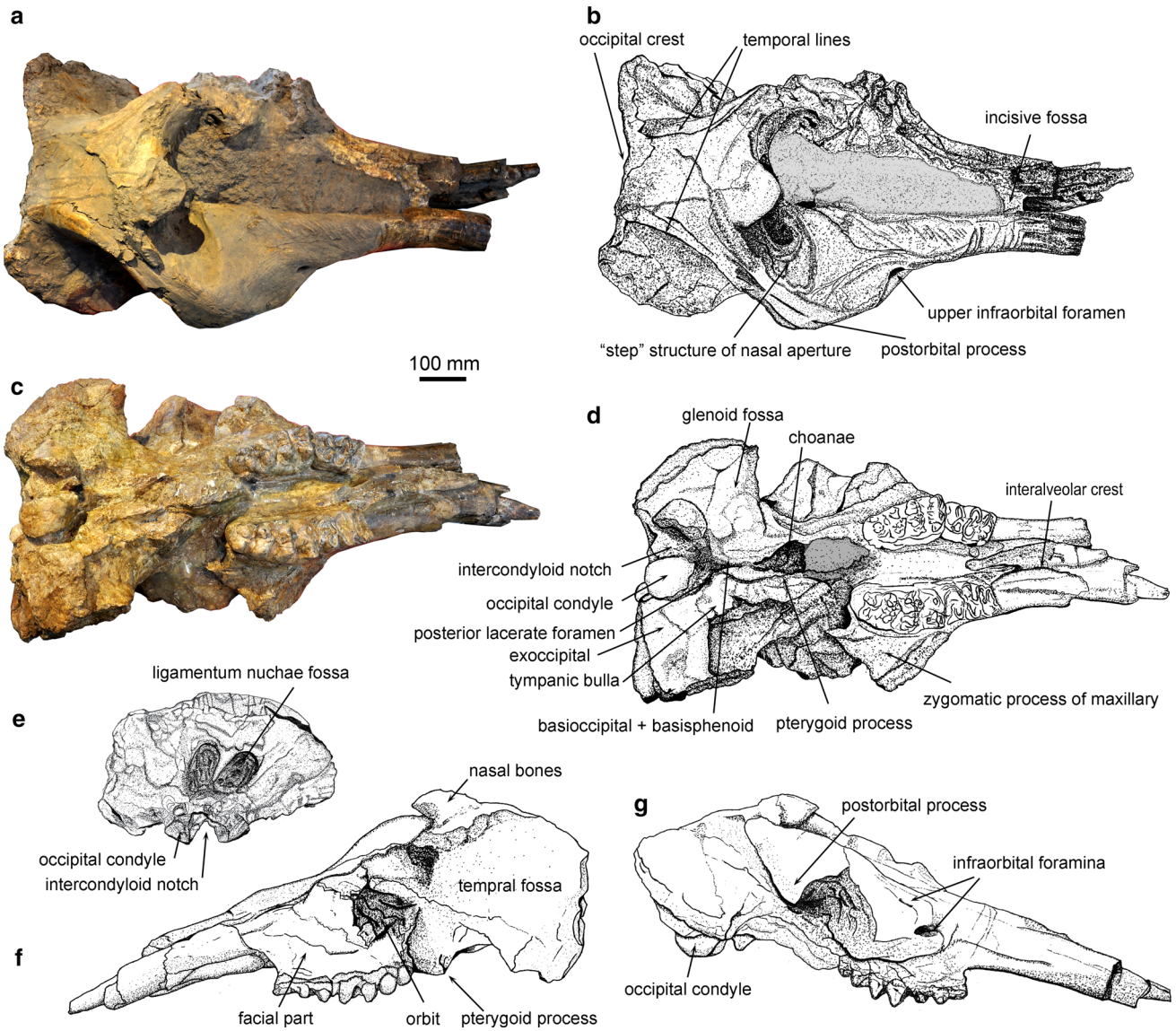

Fig. 5 Cranium of *Gomphotherium* cf. *subtapiroideum* (IVPP V3084) from Lengshuigou, Lengshuigou Formation. **a** Dorsal view; **b** sketch of **a**; **c** ventral view; **d** sketch of **c**; **e** sketch of posterior view; **f** sketch of left lateral view; **g** sketch of right lateral view

Gomphotherium shensiensis Chang and Zhai, 1978, pl. 21, Fig. 2

Gomphotherium shensiensis Chang and Zhai, 1978 Tobien et al. 1986, Fig. 13

partim *Choerolophodon* sp. Tobien et al. 1986, Fig. 23

non Gomphotherium cf. *shensiensis* Chang and Zhai, 1978 Chen 1988, pl. I, Figs. 1–3; pl. II, Figs. 1–3.

Lectotype of G. subtapiroideum right M2 and M3 [NHMW 3870 ex 1882 (A4135)], see Schlesinger 1917: pl. 7, Fig. 3. The lectotype was chosen by Osborn (1936, p. 394).

Paralectotypes of G. subtapiroideum incomplete maxillary with right M1, DP4, P4 and left DP4, DP3, P4 [NHMW C 3874 ex 1882 (A4137), see Schlesinger 1917: pl. 3 Figure 2, pl. 4 Figure 1]; right m3 (NHMW, not numbered, see Schlesinger 1917: pl. 7 Figures 1, 2); left M3 (NHMW, not numbered, Schlesinger 1917: p. 31, Fig. 3). See Osborn (1936, p. 394).

Type locality and horizon of G. subtapiroideum lignites of Vordersdorf near Eibiswald, Styria, Austria, Middle Miocene, MN5 (Göhlich 2010).

Stratigraphic and geographic distribution of G. subtapiroideum central and probably also Western Europe, Early Miocene to earlier Late Miocene, MN5 (Eibiswald, Sandelzhausen) to MN8/9 (Massenhausen, Göhlich 1998); West Asia, Middle Miocene (Turkey) (Mayda 2014).

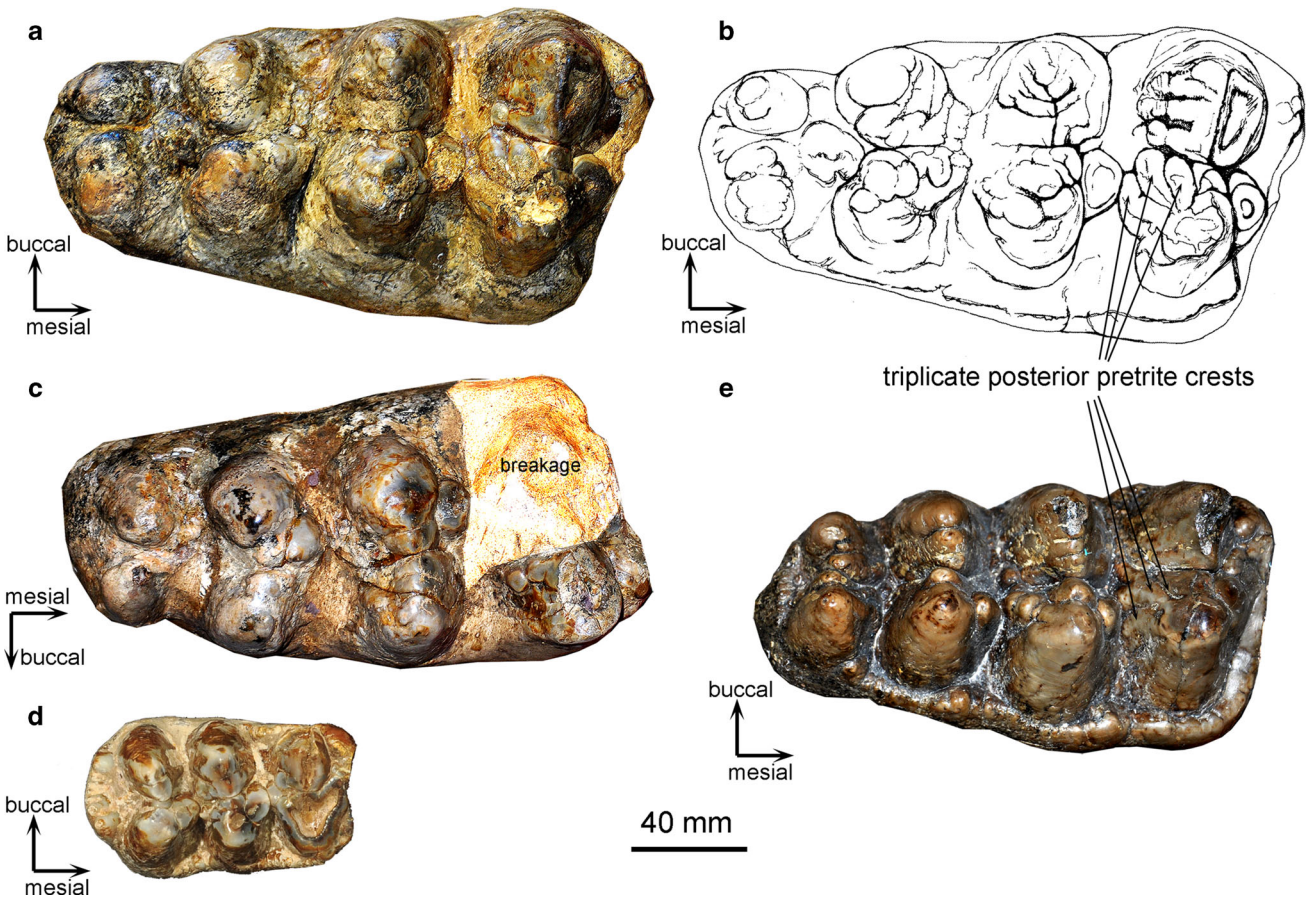

Fig. 6 Teeth of *Gomphotherium* cf. *subtapiroideum* and comparison to the lectotype of *G. subtapiroideum*, all in occlusal view. **a** Right M3 (IVPP V3084), **b** sketch of **a**; **c** left M3 (IVPP V3084); **d** right M1 (IVPP V5576); **e** right M3 [NHMW 3870 ex 1882 (A4135), the lectotype of *G. subtapiroideum* in NHMW]

Referred material of G. cf. subtapiroideum IVPP V3084, a relatively complete adult cranium. Both zygomatic arches and most apical parts of the upper tusks are broken. M2 is deeply worn and M3 is in use. This specimen is from the Lengshuigou Formation of Lengshuigou, Shaanxi Province (Chang and Zhai 1978), Middle Miocene, MN6 (Qiu and Qiu 1995). IVPP V5576.8, a right M1, moderately worn. This specimen is from the Hongliugou Formation of Heijiagou, Ningxia Province (Chen 1978), possibly corresponding to MN7/8.

Description IVPP V3084, dorsal view (Fig. 5a, b): The occipital crest is slightly anteriorly concave. The temporal lines that extend anteromedially from both lateral flanges of the occipital are intensely convergent. They run parallel along both lateral margins of the dorsal plate of the neurocranium and gradually diverge toward the postorbital processes. The dorsal plate of the neurocranium is rectangular and the free ends of the nasal bones are short and blunt. The left postorbital process is damaged and the right one is much more anterior than the superior rim of the nasal aperture. The nasal aperture is very broad with a clear lateral step. This feature is also seen in *G. angustidens* and more derived forms, but is missing in the members of *G. annectens* group (Tassy 1994, 2013). The prenasal part is vast, with a rough surface area for attachment of the *m. maxillo-labialis*; however, the insertion for the mesethmoid cartilage is not clear because of the destruction of the left premaxilla. The right upper infraorbital foramen is distantly anterior to the orbital rim and is at the base of the alveolar sockets of the premaxillae. The lateral borders of the alveolar sockets are convergent in the middle and redivergent at the opening of the tusks (indicating the specimen is male). The incisive fossa is narrow and long.

Ventral view (Figs. 5c, d, 6a–c): the ventral structures are not clear as a result of poor preservation. Both occipital condyles are bean-shaped and converge anteriorly, showing a triangular intercondyloid notch. The basioccipital is acutely tapering, and is fused with the basisphenoid; however, the fusion of the two bones cannot be distinguished. The exoccipital lateral to the occipital condyle is strong and raised. The glenoid fossa is broad and smooth, having an anterior slop that is inclined dorsally. The tympanic bulla is not laterally

Table 2 Cranial measurements (in mm, after Tassy 2013) of *Gomphotherium* cf. *subtapiroideum* (IVPP V3084)

Maximal length measured from the occipital border (1)	928
Length of cerebral part (2)	312
Length of premaxilla (3)	583
Length of incisive fossa (4)	536
Length of nasal bones from the tip to the upper border of the nasal fossa (5)	72
Maximal supraorbital width (6)	525
Posterior rostral width (as measured between the infraorbital foramina) (7)	262
Anterior rostral width (8)	206
Width of nasal bones at the upper border of the nasal fossa (9)	117
Width of nasal fossa (10)	337
Minimal cerebral width between temporal lines (11)	161
Maximal length measured from the condyles (12)	837
Length of zygomatic arch measured from the processus zygomaticus of the maxilla to the posterior border of the glenoid fossa (13)	–
Length of orbitotemporal fossa measured at the level of the zygomatic arch (14)	192
Palatal length from the anterior grinding tooth to the choanae (15)	584
Length of basicranium from the choanae to the foramen magnum (16)	290
Thickness of processus zygomaticus of the maxilla (17)	186
Maximal cranial width across the zygomatic arches (18)	–
Width of basicranium between the lateral borders of the glenoid fossae (19)	–
Maximal width of choanae (20)	–
Internal maximal width of the palate (21)	104
External maximal width of the palate (22)	266
Internal width of the palate measured at the anterior grinding teeth (23)	80
Minimal palatal width between the inter-alveolar cristae (maxillary ridges) (24)	57
Sagittal height of occipital (25)	229
Occipital width (26)	606
Height of premaxilla (27)	115
Facial height measured at the anterior grinding tooth (28)	189
Height of the maxilla ventral to the processus zygomaticus (29)	65
Height of the orbit (30)	98
Cranial height measured from the top of the cranium to the pterygoid process (31)	406
Length of basicranium from the condyles to the pterygoid process (32)	370
Facial length measured from the tip of the rostrum to the pterygoid process (33)	553
Length of the orbitotemporal fossa measured from the squamosal to the anterior border of the orbit (34)	299
Mid-cranial length measured from the external auditory meatus to the ventral border of the orbit (35)	366
Mid-cranial height measured from the pterygoid process to the dorsal border of the orbit (36)	309

expanded. A depression along the posteromedial border of the bulla represents the posterior lacerate foramen (*foramen metoticum*). The anteromedial angle of the tympanic bulla (in which the muscular process is embedded) extends anteriorly to join the pterygoid process of the alisphenoid. The choanae are filled with sediment. The M2 is deeply worn. The right M3 is just entirely erupted while the left one seems not entirely erupted; however, the left maxillary tuberosity is broken, showing the posterior end of the left M3. The two teeth rows are slightly convergent anteriorly, showing a narrow, flat palate. The zygomatic process of the maxillary is triangular, not strongly laterally expanded. The ventral plate of the alveolar sockets is fragmentary, only showing a medially convex interalveolar crest.

Posterior view (Fig. 5e): as in other elephantiforms, the occipital surface of the specimen is vast and fan-shaped. However, it is relatively low and deformed to the right side as a result of vertical pressure. The occipital condyles are triangular with a sharp intercondyloid notch between the condyles. The ligamentum nuchae fossa is rounded, rotated to the right side by deformation, and separated medially by a vertical, thin crest.

Lateral views (Fig. 5f, g): in left lateral view (Fig. 5f), the cranium is undeformed. However, the left orbital area

and the left maxillary tuberosity are damaged. The neurocranium is arched. The free end of the nasal bone protrudes anteriorly. The temporal fossa is broad and fan-shaped. The external auditory meatus is damaged and the occipital condyle cannot be observed in this view. The basicranium is not erected. The facial part is relatively low and strongly anteriorly elongated (lower and more elongated than that of *G. angustidens*, see Tassy 2013: Fig. 15). The anterior rim of the orbit is approximately at the level of the anterior part of the m3. The alveolar sockets are straight and slightly ventrally declined. In right lateral view (Fig. 5g), the cranium is flat as a result of vertical pressure. The occipital condyle is not protruded. The postorbital processes are large. The lower infraorbital foramen is just anterior to the zygomatic process of the maxillary, and the upper infraorbital foramen is at the anterodorsal margin of the orbit. The anterior rim of the orbit is approximately at the level of the anterior part of the m3 and the postorbital process of the frontal (*processus zygomaticus frontalis*) is clearly behind the dental arch.

Upper tusks only the most proximal part of each tusk is preserved. The cross-section is oval and no enamel band remains.

M2 both M2 are deeply worn, especially for the first two lophs. The second pretrite trefoil is complete. The third loph is chevron-shaped, lacking the posterior pretrite central conules. The posterior cingulum is composed of a series of conelets that links the third pretrite half lophs.

M3 (Fig. 6a–c): the left M3 lacks the first anterior pretrite half loph, and the right M3 is complete. It is composed of four lophs with the first loph being the widest. The interlophs are relatively anteroposteriorly wide. The cusps are relatively rounded and the boundaries of the crown elements are not very clear. The first pretrite half loph is complicated. The first anterior pretrite central conule is large and the first mesoconelet is small. The first posterior central conule is triplicate, showing three parallel crests that extend from the pit of the main cusp to the valley. The first posttrite half loph is transversely crest-like with three non-prominent crests running along the posterior slope of the posttrite half loph. The second anterior pretrite central conule is large. The second posterior pretrite central conule is not well developed. It is crest-like and runs from the main cusp (right M3) or the mesoconelet (left M3) to the valley. The second mesoconelet is small. The second posttrite half loph is subdivided into three to four conelets, but the posttrite posterior crests are not prominent. The third loph is chevron-shaped. The third pretrite mesoconelet is moved anteriorly to fuse with the anterior pretrite central conule, lacking the posterior central conule, and the third posttrite half loph is composed of only a mesoconelet and a main cusp. The fourth loph is composed of two strong cusps. An anterior pretrite central conule also appears to be present. Cingula are present around the anterior, posterior, lingual rims, and the buccal rims of the first loph of the tooth. However, no conelets arise from the posterior cingulum.

IVPP V5576.8 (Fig. 6d) is a right M1 composed of three lophs. The posttrite half lophs are anteroposteriorly compressed, subdivided, and crest-like. The interlophs are relatively anteroposteriorly wide. The first loph is deeply worn. The anterior pretrite central conule is crest-like, and runs to the anterior cingulum. The first posterior pretrite central conule is small. The first posterior posttrite central crest is also present. The second loph is moderately worn. The second anterior pretrite central conule is large and the posterior one is much smaller. The second posterior posttrite central crest is also present. The third anterior pretrite central conule is large, subdivided, and the posterior one is absent. The third pretrite mesoconelet is small. Cingula around the anterior, posterior, and lingual margins are strong, and cementum is weak.

Discussion the Lengshuigou cranium is not well preserved, and the detailed structures are unclear. However, the main characters are typical gomphotheriid. The neurocranium is dorsally arched, and the basicranium is not erect. The facial part of the Lengshuigou cranium is lower and more anteriorly elongated than *G. angustidens*, and to this extent, the Lengshuigou cranium is similar to that of *G. annectens* (Tassy 1994, Fig. 2C). However, the opening of the nasal aperture is very broad, showing a clear lateral step. This feature is also seen in *G. angustidens* and more derived forms, but is missing in *G. annectens* (Tassy 1994, 2013). The remaining proximal part of the upper tusks lacks an enamel band, which is why Tobien et al. (1986) retained *G. shensiensis* as a valid species. However, as Tassy (2014) pointed out, in *G. angustidens* from En Péjouan, growth of the enamel bands has ceased by the time M3 is in use. As a result, enamel bands may possibly be absent on the most proximal part of a tusk at this ontogenetic age. This may also be true for the Lengshuigou specimen. Thus, lacking enamel bands may not be a true character of the Lengshuigou material. Based on the molar pattern (see below), we refer to the Lengshuigou cranium as a similar species of another European species of the *G. angustidens* group—*G. subtapiroideum*, the validity of which has long been debated, but was recently proven by Göhlich (1998, 2010). However, the cranium of *G. subtapiroideum* is yet unknown.

The M3 of the Lengshuigou material shows a slight tendency to develop crest-like lophs and central conules. The interlophs are relatively anteroposteriorly wide. The first and second posttrite half lophs are subdivided into three or four conelets. They are transversely arranged and

crest-like. The first and second posterior pretrite central conules are also crest-like. The first posterior posttrite crests are developed (the most buccal of these crests is usually termed the zygodont crest: see Tobien 1975; Göhlich 2010). These features are consistent with *Gomphotherium subtapiroideum*. The most peculiar feature of the M3 is the triplication of the first posterior pretrite crest. This is an unusual feature; however, it is very similar to the type specimen of *G. subtapiroideum*, in which the same element is also tripled (Fig. 6e). Compared with the type specimen of *G. subtapiroideum*, the Lengshuigou material shows slightly more bunodont features, and weaker cingula. Furthermore, the cranium of *G. subtapiroideum* is yet unknown to us. Therefore, we referred to the Lengshuigou specimen as *G.* cf. *subtapiroideum*. Moreover, compared with the syntypes of *G. inopinatum*, since the molar's morphology of the two species are similar (Wang 2014), the M3 of the Lengshuigou specimen possesses a more complete fourth loph, more crest-like posttrite half lophids, and more developed pretrite central conules (Borissiak and Belyaeva 1928). Thereby, as *G. angustidens*, *G. subtapiroideum* (or phylogenetically related species) had also penetrated into the eastern part of the Palearctic. This high similarity of *Gomphotherium* at the species level across the Palearctic should be noted.

The M1 (V5576.8) is included with nine m1 or m2 teeth, all of which are together numbered as V5576 (7 *P. grangeri* and 2 *Gomphotherium*, in which V5576.8 is a *Gomphotherium* cf. *subtapiroideum*). The seven *P. grangeri* teeth were described by Chen (1978). However, she did not mention the two *Gomphotherium* teeth, which may have been collected from the same locality (Heijiagou) as the teeth of *P. grangeri*. The crown of the M1 is very different from that of *Platybelodon*, in which the tooth is narrower with stronger posttrite central conules, stronger pseudoanancoidy, stronger cementum, and weaker cingulum. Tobien et al. (1986) attributed V5576.8 to *Choerolophodon* sp. However, in V5576.8, no strong chevron-shapedness, choerolophodonty, ptychodonty, and cementum are present, as in typical *Choerolophodon*. The subdivision, anteroposterior compression of the posttrite lophs, and open interlophs are in good agreement with the features of *G.* cf. *subtapiroideum*. As this specimen may have been contemporary with *P. grangeri*, the temporal range of *G.* cf. *subtapiroideum* may extend to MN7/8 in East Asia.

Conclusions

In this paper, we describe several specimens of *Gomphotherium* from the Lower and Middle Miocene of China that have previously been studied by other colleagues and that are systematically revised here: *G. connexum* from the type locality Diaogou, *G. shensiensis* from Lengshuigou, *G.* cf. *shensiensis* and *Gomphotherium* sp. from the Junggar Basin, and a *Gomphotherium* specimen from Hejiagou. We conclude that *G. connexum* is a close relative of European *G. angustidens* and belongs to the *G. angustidens* group sensu Tassy (1985). Specimens formerly determined as *Gomphotherium* cf. *shensiensis* and *Gomphotherium* sp. from the Junggar Basin are identified here as *G. connexum*. They show some more derived features, such as larger size and heavier cementum, than the type material of *G. connexum*. We consider *Gomphotherium shensiensis* is a similar species of European *G. subtapiroideum*. This revision of Chinese *Gomphotherium* specimens shows a high similarity of *Gomphotherium* on the species level between eastern and western Eurasia. We think *G. connexum* and *G. subtapiroideum* dispersed across the Palearctic during the Middle Miocene, however, with slightly variation.

Acknowledgments We thank P. Tassy and U.B. Göhlich for much help in comparing European specimens and providing literature, and Z.-X. Qiu, G.-F. Chen, T. Deng, Z.-D. Qiu, J. Ye, and J.-J. Zheng for useful advice and various types of assistance. We thank G. Markov and two anonymous reviewers for many suggestions to improve the article. We thank D. Wolf and M. Aiglstorfer for translating the abstract to German. This work was supported by the National Basic Research Program of China (Grant Number 2012CB821900), the Chinese Academy of Sciences (Grant Number XDB03020104), the National Natural Science Foundation of China (Grant Numbers 41372001, 41430102, 41202017), and the Key Laboratory of Economic Stratigraphy and Palaeogeography, Chinese Academy of Sciences (Nanjing Institute of Geology and Palaeontology).

References

Burmeister, H. 1837. *Handbuch der Naturgeschichte. Zum Gebrauch bei Vorlesungen*. Berlin: Enslin.

Borissiak, A.A., and E. Belyaeva. 1928. *Trilophodon* (*Serridentinus*?) *inopinatus* n. sp. from the Jilančik Beds of the Turgai Region. *Bulletin de l'Académie des Sciences de l'URSS, Classe des Sciences Physico-Mathématique. Leningrad* 241–252.

Chang, H.-C., and R.-J. Zhai. 1978. Miocene mastodonts of Lantian and Lintung, Shensi. *Professional Papers of Stratigraphy and Palaeontology* 7: 136–142 (Chinese 136–141; English 141–142).

Chen, G.-F. 1978. Mastodont remains from the Miocene of Zhongning–Tongxin area in Ningxia. *Vertebrata PalAsiatica* 16(2): 103–110 (Chinese).

Chen, G.-F. 1988. Mastodont remains from the Miocene of Junggar Basin in Xinjiang. *Vertebrata PalAsiatica* 26(4): 265–277 (Chinese 265–273; English 274–277).

Chow, M.C., and Y.-P. Zhang. 1974. *Chinese fossil elephantoids*. Beijing: Science Press (Chinese).

Cope, E.D. 1884. The extinct Mammalia of the valley of Mexico. *Proceedings of the American Philosophical Society* 22: 1–21.

Depéret, C. 1897. Découverte du *Mastodon angustidens* dans l'étage cartennein de Kabylie. *Bulletin de la Société géologique de France* 3(25): 518–521.

Falconer, H. 1857. On the species of mastodon and elephant occurring in the fossil state in Great Britain. Part I. *Mastodon*. *Quarterly Journal of the Geological Society of London* 13: 307–360.

Frick, C. 1933. New remains of trilophodont-tetrabelodont mastodons. *Bulletin of the American Museum of Natural History* 56: 505–652.

Hay, O.P. 1922. Further observations on some extinct elephants. *Proceedings of the Biological Society of Washington* 35: 97–101.

Illiger, C.D. 1811. *Prodromus systematis mammalium et avium additis terminis zoographicis uttriusque classis*. Berlin: Salfeld.

Gasparik, M., and G.N. Markov. 2009. *Gomphotherium* "*annectens* group" (Proboscidea) in Hungary. *Fragmenta Palaeontologica Hungarica* 27: 73–79.

Göhlich, U.B. 1998. Elephantoidea (Proboscidea, Mammalia) aus dem Mittel- und Obermiozän der Oberen Süßwassermolasse Süddeutschlands: Odontologie und Osteologie. *Münchner Geowissenschaftliche Abhandlungen* 36: 1–245.

Göhlich, U.B. 2007. Gomphotheres (Proboscidea, Mammalia) from the Early-Middle Miocene of Central Mongolia. In *Oligocene–Miocene vertebrates from the valley of lakes* (*Central Mongolia*)*: morphology, phylogenetic and stratigraphic implications*, ed. G. Daxner-Höck. *Annalen des Naturhistorischen Museums in Wien* 108A: 271–289.

Göhlich, U.B. 2010. The Proboscidea (Mammalia) from the Miocene of Sandelzhausen (southern Germany). *Paläontologische Zeitschrift* 84(1): 163–204.

Hopwood, A.T. 1935. Fossil Proboscidea from China. *Palaeontologia Sinica, Series C* 9: 1–108.

Mayda, S. 2014. Review of the Late Neogene Proboscideans from Turkey. In *Abstract book of the VIth international conference on mammoths and their relatives, 5–12 May 2014, Grevena-Siatista*, eds. D.S. Kostopoulos, E. Vlachos, and E. Tsoukala, Scientific Annals of the School of Geology, Aristotle University of Thessaloniki, special issue 102: 125–126.

Osborn, H.F. 1923. New subfamily, generic, and specific stage in the evolution of the Proboscidea. *American Museum Novitates* 99: 1–4.

Osborn, H.F. 1924. *Serridentinus* and *Baluchitherium*, Loh Formation, Mongolia. *American Museum Novitates* 148: 1–5.

Osborn, H.F. 1932. *Trilophodon cooperi* n. sp. of Dera Bugti, Baluchistan. *American Museum Novitates* 393: 1–6.

Osborn, H.F. 1936. *Proboscidea: a monograph of the discovery, evolution, migration and extinction of the mastodonts and elephants of the world*. New York: The American Museum Press.

Qiu, Z.-D., C.-K. Li, and S.-J. Wang. 1981. Miocene mammalian fossils from Xining Basin, Qinghai. *Vertebrata PalAsiatica* 19(2): 156–173 (Chinese 156–168; English 169–173).

Qiu, Z.-X., and Z.-D. Qiu. 1995. Chronological sequence and subdivision of Chinese Neogene mammalian faunas. *Palaeogeography, Palaeoclimatology, Palaeoecology* 116: 41–70.

Schlesinger, G. 1917. Die Mastodonten des K. K. naturhistorischen Hofmuseums. *Denkschriften des K. K. Naturhistorischen Hofmuseums, Geologisch-paläontologische Reihe* 1: 1–231.

Sanders, W.J., E. Gheerbrant, J.M. Harris, H. Saegusa, and C. Delmer. 2010. Proboscidea. In *Cenozoic mammals of Africa*, ed. L. Werdelin, and W.J. Sanders, 161–251. Berkeley: University of California Press.

Shoshani, J., and P. Tassy. 2005. Advances in proboscidean taxonomy & classification, anatomy & physiology, and ecology & behavior. *Quaternary International* 126–128: 5–20.

Tasnádi Kubacska, A. 1939. *Trilophodon angustidens* Cuv. forma *praetypica* koponyamaradványa Zagyvapálfalváról. *Annales Musei Nationalis Hungarici, Pars Mineralogica, Geologica et Palaeontologica* 22: 154–164.

Tassy, P. 1977. Le plus ancien squelette de gomphothère (Proboscidea, Mammalia) dans la Formation Burdigalienne des sables de l'Orléanais France. *Mémoirs du Muséum National d'Histoire Naturelle (N. Sér) C* 37: 1–51.

Tassy, P. 1985. La place des mastodontes Miocènes de l'ancien monde dans la phylogénie des Proboscidea (Mammalia): hypothèses et conjectures. 861 p., unpubl. D.Sc. these, UPMC, Paris.

Tassy, P. 1994. Gaps, parsimony, and early Miocene elephantoids (Mammalia), with a re-evaluation of *Gomphotherium annectens* (Matsumoto, 1925). *Zoological Journal of the Linnean Society* 112: 101–117.

Tassy, P. 2013. L'anatomie cranio-mandibulaire de *Gomphotherium angustidens* (Cuvier, 1817) (Proboscidea, Mammalia): Données issues du gisement d'En Péjouan (Miocène moyen du Gers, France). *Geodiversitas* 35(2): 377–445.

Tassy, P. 2014. L'odontologie de *Gomphotherium angustidens* (Cuvier, 1817) (Proboscidea, Mammalia): Données issues du gisement d'En Péjouan (Miocène moyen du Gers, France). *Geodiversitas* 36(1): 35–115.

Tassy, P., F. Goussard, and M.G. Sanz. 2013. The status of *Mastodon angustidens pygmaeus* Depéret, 1897 (Proboscidea, Mammalia): The contribution of X-ray tomography. *Geobios* 46: 329–334.

Tobien, H. 1972. Status of the genus *Serridentinus* Osborn 1923 (Proboscidea, Mammalia) and related forms. *Mainzer Geowissenschaftliche Mitteilungen* 1: 143–191.

Tobien, H. 1973. On the evolution of mastodonts (Proboscidea, Mammalia). Part 1: The bunodont trilophodont groups. *Notizblatt des Hessischen Landesamtes für Bodenforschung zu Wiesbaden* 10: 202–276.

Tobien, H. 1975. The structure of the mastodont molar (Proboscidea, Mammalia). Part 2: The zygodont and the zygobunodont patterns. *Mainzer Geowissenschaftliche Mitteilungen* 5: 143–225.

Tobien, H., G.-F. Chen, and Y.-Q. Li. 1986. Mastodonts (Proboscidea, Mammalia) from the late Neogene and early Pleistocene of the People's Republic of China. Part I: Historical account: The genera *Gomphotherium*, *Choerolophodon*, *Synconolophus*, *Amebelodon*, *Platybelodon*, *Sinomastodon*. *Mainzer Geowissenschaftliche Mitteilungen* 15: 119–181.

Vacek, V.M. 1877. Über österreichische Mastodonten und ihre Beziehungen zu den Maston-Arten Europas. *Abhandlungen der Kaiserlich-Königlichen Geologischen Reichsanstalt* 7(4): 1–45.

Wang, S.-Q. 2014. *Gomphotherium inopinatum*, a basal *Gomphotherium* species from the Linxia Basin, China, and other Chinese members of the genus. *Vertebrata PalAsiatica* 52(2): 183–200.

Wang, S.-Q., W. He, and S.-Q. Chen. 2013. Gomphotheriid mammal *Platybelodon* from the middle Miocene of Linxia Basin, Gansu, China. *Acta Palaeontologica Polonica* 58: 221–240.

Welcomme, J.-L. 1994. Le plus ancien crâne de proboscidien d'Europe, *Gomphotherium hannibali* nov. sp. (Proboscidea, Mammalia), du Miocène inférieur du Languedoc (France). *Comptes Rendus de l'Académie des Sciences Paris, Série II* 319: 135–140.

Ye, J., W.-Y. Wu, X.-J. Ni, S.-D. Bi, J.-M. Sun, and J. Meng. 2012. The Duolebulejin Section of northern Junggar Basin and its stratigraphic and environmental implication. *Science China: Earth Sciences* 42: 1523–1532 (Chinese).

Young, C.C., and M.N. Bian. 1937. Cenozoic geology of the Kaolan-Yungteng area of Central Kansu. *Bulletin of the Geological Society of China* 16: 221–260.

Zhai, R.J. 1961. On a collection of Neogene mammals from Ching-An, Eastern Kansu. *Vertebrata PalAsiatica* (3): 262–268 (Chinese 262–267; English 268).